JOURNAL OF APPLIED PHYSICS **113**, 054316 (2013)

The increase in conductance of a gold single atom chain during elastic elongation

F. Tavazza, S. Barzilai,[a] D. T. Smith, and L. E. Levine
Material Measurement Laboratory, National Institute of Standards and Technology, 100 Bureau Drive, Stop 8553, Gaithersburg, Maryland 20899, USA

(Received 16 November 2012; accepted 22 January 2013; published online 7 February 2013)

The conductance of monoatomic gold wires has been studied using *ab initio* calculations and the transmission was found to vary with the elastic strain. Counter-intuitively, the conductance was found to increase for the initial stages of the elongation, where the structure has a zigzag shape and the bond angles increase from ≈140° toward ≈160°. After a certain elongation limit, where the angles are relatively high, the bond length elongation associated with a Peierls distortion reverses this trend and the conductance decreases. These simulations are in good agreement with previously unexplained experimental results. © *2013 American Institute of Physics*. [http://dx.doi.org/10.1063/1.4790379]

I. INTRODUCTION

Gold nanowires are extremely ductile and thin down to single atom chains (SACs) during tensile deformation. This unusual ability has attracted a great deal of attention from a basic science viewpoint since SACs exhibit remarkable electrical and structural properties. Gold SACs also have great potential in applied fields such as nanoelectronics. Many experimental[1–10] and theoretical[11–24] studies have been carried out to explain the SAC formation and its electrical characteristics. Using density-functional theory (DFT) simulations, it was found that during the nanowire elongation, the arrangement of the gold atoms changes from three-dimensional (3D) phases to a variety of two-dimensional (2D) phases and finally to SACs, which elongate gradually from one up to about nine atoms in the chain.[24,25] The electrical studies revealed that during the nanowire elongation, the conductance decreases in a step-like fashion due to structural rearrangements that affect the number of available conductance channels.[26,27] Within each step, a variety of electrical behaviors were found experimentally and explained using conductance simulations.[7,25] After the formation of the SAC, small fluctuations (≈15%) in the conductance were experimentally observed during elongation.[7] Several theoretical studies[21,28,29] demonstrated that these fluctuations occur when a single gold atom transitions from the 2D part of the nanowire to the SAC. This movement increases the number of atoms in the SAC by one and changes its state from even to odd and vice versa. It was found[28] that these states have different transmission spectra that make the conductance higher for odd numbers of atoms in the SAC and lower for even numbers. Another effect that has been satisfactorily explained is the gradual decrease of conductivity within a "plateau" during elastic elongation, which has been attributed to bond stretching.

However, another important characteristic behavior of SACs has not yet been explained. As seen in Fig. 4 of Refs. 7 and 9, in Fig. 3 of Ref. 8 and in Fig. 1 of the present study, the measured conductance is sometimes observed to gradually *increase* during elastic elongation immediately after a Au atom in a 2D configuration suddenly inserts itself (pops) into the 1D chain. A similar conductance increase has recently been reported in tensile experiments on a single molecule of gold-1,4'-benzenedithiol in a gold break junction.[30] The authors attributed the conductance increase to a strain-induced shift of the highest occupied molecular orbital (HOMO) towards the Fermi level of the electrodes. This mechanism is not applicable to a Au SAC since the HOMO is already at the Fermi level. In this study, DFT and conductance simulations are used to investigate the origins of this counter-intuitive conductance behavior in Au SACs. For the conductance calculations, we elongated chains of different lengths and investigated the corresponding changes in the conductance. It is well known[21,28,29] that odd-even oscillations in the conductance are observed as the number of atoms in the SAC increases. However, in this work, the primary interest is in how the conductance increases with elastic elongation, and this effect occurs equally for all chain lengths. Therefore, even though different SAC lengths were investigated (from 2 atoms to 7 atoms), only results for 6 atom chains are discussed here. All of the findings obtained for this length apply to other SAC lengths as well. Understanding all of the mechanisms that control the conductance in atomic-scale wires is important both from a basic science standpoint and for applications in nanoelectronics and nanodevices.

II. METHODOLOGY

Several different types of simulations are reported, including tensile deformation of two dimensional and SAC Au configurations, with corresponding quantum conductance calculations. These simulations are then compared to experimental results.

The calculations performed to elongate the nanowires were carried out in the framework of density functional theory (DFT) using the DMol^3 code.[31–33] This code employs localized basis sets, which make them fast and particularly well suited for cluster calculations. We used a real-space

[a]On sabbatical leave from the Nuclear Research Center NEGEV.

cutoff of 4 Å and a double-zeta, atom-centered basis set (dnd). The exchange-correlation potential was treated within the Perdew-Burke-Ernzerhof (PBE) generalized gradient approximation (GGA) approach.[37] The ion core electrons of the Au were described by a hardness conserving semilocal pseudopotential (dspp);[38] only the outer electrons ($5s^2$ $5p^6$ $5d^{10}$ $6s^1$) were treated as valence electrons. The geometry optimization was performed using a conjugate gradient approach based on a delocalized internal coordinate scheme.[39,40] The system was considered converged when the change in total energy dropped below 10^{-4} eV and the maximum displacement dropped below 10^{-4} Å. For the SAC calculations, the simulation cell only had periodicity along the SAC axis (z axis), and $1 \times 1 \times 10$ Monkhorst-Pack k-points[41] were used during the relaxations. Details on how the actual elongation of the wire was performed are given in Ref. 24.

The conductance calculations were performed at zero bias using a non-equilibrium Green's function technique based on the Landauer formalism,[34] and local density approximation (LDA) approach[42] with a double-zeta polarized (DZP) numerical basis set,[43] as implemented in the ATK package.[17,35,36] The system was divided into three regions: the left and right Au electrodes and the central scattering region. For the latter, we used the atomic configurations obtained by the elongation. In this work, as in Ref. 44, triangular Au electrodes were used. More details on how the conductance is computed are given in Ref. 44. Details on the 2D chain simulations may be found in Ref. 24.

In this paper, the results from four kinds of simulations are examined. In the first two sets of simulations, an existing SAC is elongated. At each elongation step, the SAC is relaxed either by allowing motion only along the chain axis or by allowing a full 3D relaxation. In the first instance, we are forcing the SAC into a linear configuration; in the second instance, a more realistic non-linear configuration was found, which is referred to as a monoatomic "zigzag" in this work. As discussed in greater detail in Sec. III, the angles between the atoms in this "zigzag" structure ranged from about 135° to about 175°, depending on the degree of elongation. To clarify the effect of the angle on the conductance, in the third simulation, we calculate the conductance for several SACs having fixed geometries without relaxation but with different bond angles. In the last simulation, we started from a more realistic 2D structure, and elongated it until a SAC was formed. We then continued elongating the wire and analyzed the conductance properties of the complete system (SAC + remaining 2D structure). This simulation is completely equivalent to those described in Ref. 24. This more general approach allows the SAC to elongate, not only just through the elongation of the existing bonds but also through the addition of new atoms to the chain itself.

Historically, many experiments have probed electrical conduction in Au nanowires by rapidly making and breaking numerous contacts, then generating histograms of observed conduction values.[1–4,7] Instead, we have developed a feedback-stabilized break junction (FSBJ) instrument,[45] with exceptional mechanical stability, and used it to draw individual Au nanowires and single atom chains quasistatically at 4 K while measuring the elongation and conductivity of the wire. At the heart of the FSBJ is a fiber-optic Fabry-Perot interferometer of our own design[46] that has been optimized for dc and low-frequency stability. In this system, a Au break junction is formed between the tip of a Au wire and a Au flat; a 5 mV bias is applied to measure the conductance. Parallel to the Au wire, a Fabry-Perot interferometer cavity is formed between the cleaved end of an optical fiber and the same Au flat used for the break junction. The interferometer is capable of detecting changes in the position of the Au flat with 2 pm resolution, and its output is used to stabilize the cavity length with the same precision. It is this level of long-term stability in the position of the Au tip relative to the Au flat that makes the experimental results described here possible.

III. RESULTS

Using the FSBJ, we have performed hundreds of Au break-junction experiments at 4 K using several different Au tips and multiple contact locations on a given Au flat. We focus here on 11 experimental results that exhibited low conductance contacts ($G \approx G_0$, where $G_0 = 2e^2/h$, with e the electron charge and h Planck's constant) and are slowly drawn out until they break. This drawing process typically took from 1 s to 30 s. Representative examples of our findings are displayed in Figs. 1(a) and 1(b). Figs. 1(a) and 1(b) show the unexplained conductance increase that sometimes occurs after an atom pops into the SAC from the gold nanowire (GNW). This phenomenon is rarely distinguished in the experiments and the ability to distinguish it depends on the stability of the experimental system and on the structural stiffness of the SAC grips. As can be seen (Figs. 1(a) and 1(b)), the conductance state indicates that the GNW contains a SAC region, and the step-like change in the conductance indicates a Au atom popping-into the SAC. In Fig. 1(a), after the pop-in, the conductance drops abruptly to about 0.91 G_0 and then quickly increases to around 0.94 G_0 (at 8 Å displacement). This kind of conductance increase can also be seen in experimental results that have been published previously.[7–9] Another, longer, occurrence where the conductance of a Au SAC is observed to increase with elastic strain is shown in Fig. 1(b); here, the conductance exhibits a continuous increase from 0.936 G_0 to 0.952 G_0. The difference in the observed *rate of increase* of the conductance is discussed in the summary. Despite the counter-intuitive nature of this behavior and the importance of understanding all of the measured conductance features, this unusual behavior has never previously been explained or discussed.

As a first step in investigating the deformation of a Au SAC, we determined the zero-stress bond length for a uniformly deformed, linear SAC, i.e., a SAC where all of the bonds are the same and all of the atoms are along a straight line. Under these very simplified conditions, the zero-stress bond length was found to be about 2.62 Å. As a consequence, to explore chains under both compressive and tensile strains, we examined SACs with wire lengths from 12.4 Å to 14.7 Å, which correspond to an average bond distance from 2.48 Å to 2.94 Å in the case of a straight chain. Then, to understand the effect of the elongation process on the conductance of gold SACs, we performed two kinds of simulations. First,

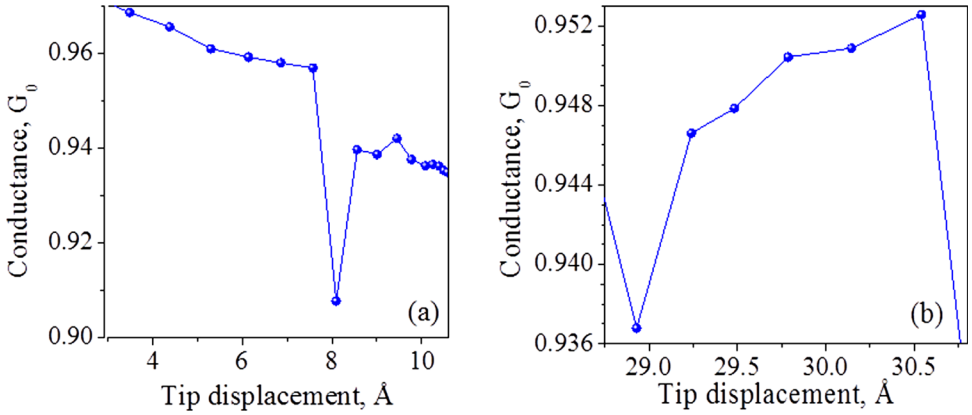

FIG. 1. Sharp (a) and gradual (b) increase of the conductance measured for 2 different wires after a Au atom popped into the SAC.

the effect of bond elongation on the conductance of SACs (Fig. 2) was studied by restricting the atoms to a linear configuration. This restriction is not entirely physical, since fully relaxed SACs exhibit at least some degree of zigzag character. Thus, our second set of simulations dropped this restriction and examined the combined effect of bond lengths and bond angles in the SAC (Fig. 3).

Fig. 2 shows the bond length (Fig. 2(a)) and conductance (Fig. 2(b)) changes that occur during the elongation of a linear SAC composed of six gold atoms. Here, the SAC was uniaxially elongated from 12.4 Å to 14.7 Å, and gold atoms were allowed to relax only within the direction of elongation. As can be seen (Fig. 2(a)), the behavior of the bonds in the SAC can be divided into two stages. Below a SAC length of 14 Å, all of the bond lengths increased linearly with elongation. Upon further elongation, three of the Au-Au bonds *decreased* in length and the remaining two bonds elongated more rapidly than before to compensate. This behavior is generally referred to as a Peierls distortion. The lengthening of the atomic separation decreases the orbital overlap causing the conductance to go down. As shown in Fig. 2(b), the SAC conductance decreased at a moderate rate until the SAC reached 14 Å. Once the Peierls distortion occurred, the slope of the conductance curve steepened by a factor of three. Thus, conductance is more sensitive to the maximal bond length than to either the average bond length or the total length of the SAC. This Peierls behavior is illustrated beautifully with the inset isosurfaces in Fig. 2(b). When the length of the SAC was more than 14 Å, the primary decrease in the electron density occurred only within the two maximal bond lengths.

Fig. 3 demonstrates the combined effect of bond length and angle changes on the conductance of a zigzag SAC structure. In this simulation, the SAC was uniaxially elongated from 12.4 Å to 14.7 Å and the gold atoms were allowed to relax both in the elongation direction and perpendicular to it. During the initial stages of the elongation towards 14 Å, the bond lengths (Fig. 3(a)), the bond angles (Fig. 3(b)), and the conductance (Fig. 3(c)) all increased. This remarkable behavior is consistent with the experimentally observed increases in conductance with elongation discussed above. Further elongation caused a slow decrease in the lengths of three bonds, a rapid increase in the other two bond lengths and a moderate increase in the bond angles. These geometric changes produced a relatively sharp decrease in the conductance, consistent with the latter stage of the linear SAC elongation shown in Fig. 2. This simulation demonstrates that both bond lengths and bond angles play an important role in controlling the conductance. Initially, conductance increases even though the increasing bond lengths would normally be expected to produce a decrease in the conductance (see Fig. 2(a)). Thus, at this stage, the increasing bond angles are the dominant factor. Beyond a SAC length of ≈ 14 Å, the bond angles change very little (Fig. 3(b)) while the lengths of two of the bonds increase significantly (Fig. 3(a)). In this regime, the elongation of the maximal bond length controls the conductance, which rapidly decreases until the bonds break.

To investigate the effect of the bond angle by itself on the conductance, two kinds of analysis were made. At first, we calculated the conductance for different bond angles from 150° to 180° on fixed atom configurations with equal bond lengths of 2.8 Å (Fig. 4(a)). Second, we used the data obtained from the previous simulation (Figs. 2 and 3) to see if this effect exists also in more realistic simulations where the bond lengths are not equal and the atoms are allowed to

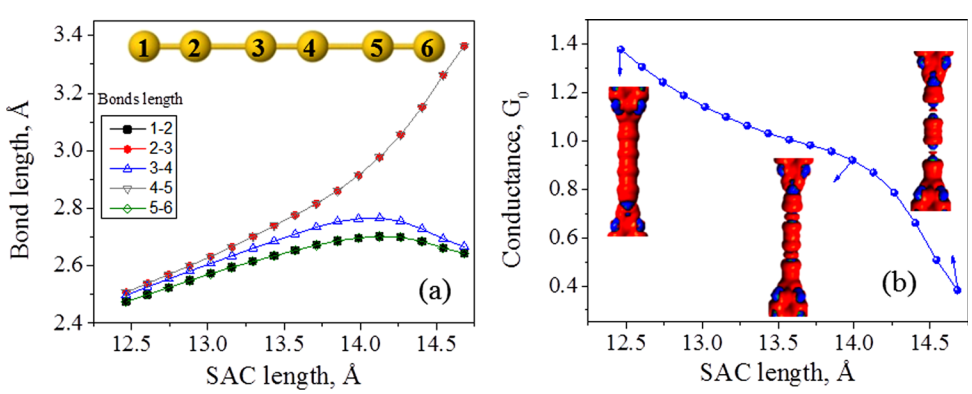

FIG. 2. The effect of elongation on the bonds lengths (a) and conductance (b) for a linear SAC. The inserted images in (b) represent a difference electron-density isosurface of 0.015 e/Å^3.

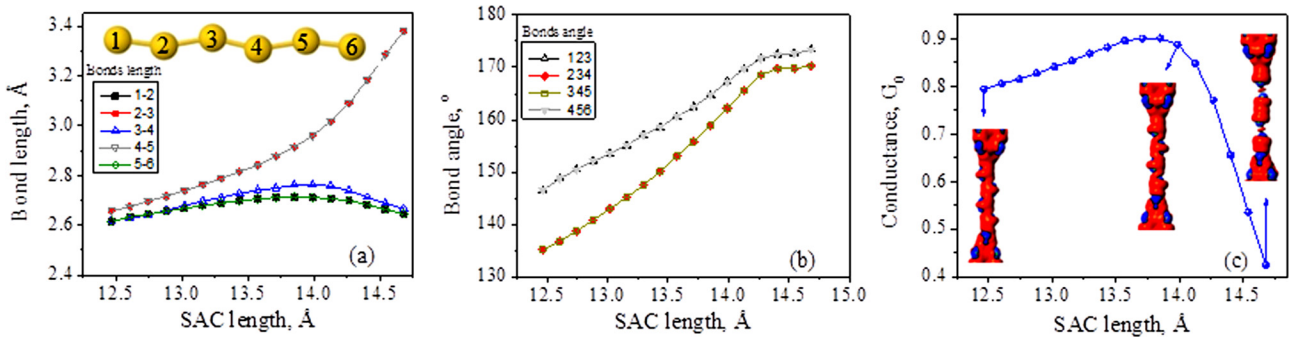

FIG. 3. The effect of elongation on the bond lengths (a), angles (b) and conductance (c) for a zigzag SAC. The inserted images in (c) represent a difference electron-density isosurface of 0.015 e/Å^3.

relax. We first fitted a polynomial function to the linear SAC simulation to obtain the dependence of the conductance on the maximal bond length (Fig. 4(c)). For the zigzag SAC simulation, we then determined the maximal bond length for each SAC length. This allowed us to obtain two conductance values for each SAC length for the zigzag SAC simulation: the wire conductance that we calculate directly from the simulation (Fig. 3(c)) and the fitted conductance from the maximal bond length (Fig. 4(c)). Fig. 4(b) shows the difference between these two conductance values. By assuming that there are no synergistic effects between the bond length and bond angles, this conductance difference describes the effect of the bond angle on the conductance. As seen in Figs. 4(a) and 4(b), the conductance smoothly increases with increasing bond angle. This mechanism dominates during the initial stages of the elongation where the maximal bond length increases very slowly (Fig. 3(a)). However, during the later stages of the elongation, the increase in the maximal bond length overcomes the effect of increasing bond angle and the wire conductance decreases.

This bond-angle effect may be understood in terms of the changing relative orientation of the conducting electron orbitals. In gold SACs, the conductance is mostly governed by the 5*d* electrons. As the angle increases, these orbitals become more aligned with the equivalent orbitals of the adjacent atom, therefore increasing the orbital overlap and the overall conductance. To strengthen our interpretation, we performed conductance simulations as described for Fig. 4(a) for Li atoms instead of gold ones. Li atoms conduct mostly with their *2s* electrons, which have no directionality. In this case, the angle increase does not affect the distance or alignment between *2s* orbitals. We found that, in the Li case, the bond angle has almost no effect on the conductance (dashed line in Fig. 4(a)).

The simulations described above explore the conductance behavior of a Au SAC as it is elastically stretched. However, experimental systems are much more complex, with thicker samples thinning to SACs and the number of Au atoms in the SAC increasing with elongation. In order to broaden our investigation to more realistic systems, we next examine what happens when a 2D nanowire evolves into a SAC during tensile deformation. The 2D system used here was studied previously[24] in earlier DFT simulations.

In this simulation, the SAC is created by bond-breaking within the starting 2D structure and, unlike the previous simulations, the number of Au atoms in the SAC increases as the deformation continues. This process affects the bond lengths, the bond angles, and the number of Au atoms in the SAC, and therefore changes the conductance. Fig. 5 shows the structural and conductance changes that occur during the elongation processes.

As can be seen in Fig. 5, the conductance decreases and increases in a cyclic manner during the elongation. The sharp conductance decrease from A→B is related to the initial formation of a SAC from the starting 2D structure. The subsequent drops from C→D and E→F are not straightforward and involve several structural changes that take place at the same time. However, for the G→H→I path, the bond angles are

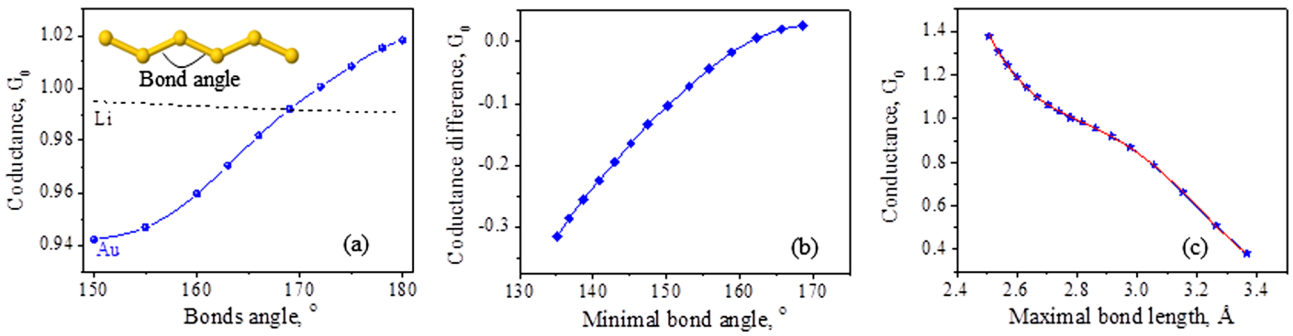

FIG. 4. The effect of bond angle on the conductance: (a) as calculated for several simulations of relaxed SACs having identical bond lengths of 2.8 Å and different bond angles, (b) as computed for the relaxed simulation and after eliminating the contribution of the maximal bonds length shown in (c). The dashed line in (a) indicates the conductance of a Li SAC having identical bond lengths of 2.8 Å.

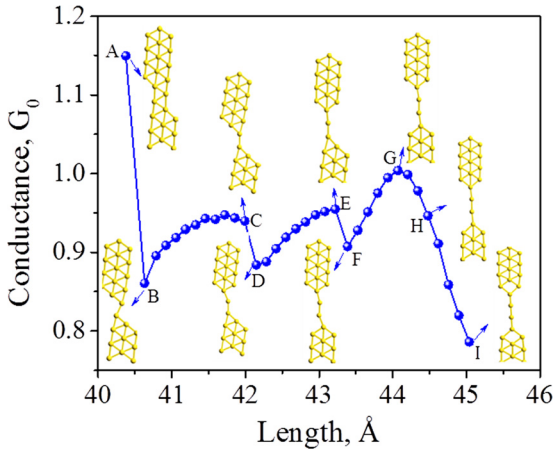

FIG. 5. Structural and conductance behavior computed for tensile deformation of a 2D GNW.

higher than 170° (and therefore have only a small effect on the conductance), the number of atoms in the SAC is constant, and the main structural change is an increase in the maximal bond length that causes the conductance to decrease. The observed increase in the conductance from B→C, D→E and F→G involves increases in both bond lengths and bond angles. As found in the earlier simulations, the increasing bond lengths suggest that the conductance should decrease, but the increasing bond angles dominate the process and cause the conductance to increase.

IV. SUMMARY AND CONCLUSIONS

The DFT and conductance simulations described above provide an explanation for the counter-intuitive increase in conductance that Au SACs sometimes exhibit during elastic elongation. This unexpected behavior has been observed in our own experiments and also in others.[7–9] The increase in conductance is attributed to the gradual increase in the bond angles that occurs when a zigzag-shaped Au SAC elongates. In the simulations, this behavior commonly appears immediately following major structural transitions such as the addition of atoms to the SAC (see Fig. 5). However, this behavior is only rarely observed in experiments. As described previously,[25] the simulated transitions produce large changes in the force on the nanowire and can even produce a SAC that is under a slight compressive rather than tensile load, thus enhancing the range of bond angles observed during stretching. In most experimental systems, the SAC evolves through an extensive ductile thinning process that leaves long, thin "grips" attached to the much smaller SAC. Thus, when a Au atom pops into the SAC, this region is immediately stretched again due to the elastic strain of the grips, and the added length of a single atom hardly affects either the force on the wire or the bond angles in the SAC. In mechanical testing terms, the experiment can have a large mechanical compliance and the assumption of strict displacement control is not valid for the SAC region. Thus, the opportunity for observing a conductance increase during SAC elongation depends upon the shape of the grips (and thus the spring constant) that develops during the experiment. In contrast, in the simulations the grips are very short, their compliance is negligible, and the conductance increase is readily observed.

[1] I. K. Yanson, O. I. Shklyarevskii, Sz. Csonka, H. van Kempen, S. Speller, A. I. Yanson, and J. M. van Ruitenbeek, Phys. Rev. Lett. **95**, 256806 (2005).
[2] M. Kiguchi, T. Konishi, and K. Murakoshi, Phys. Rev. B **73**, 125406 (2006).
[3] R. Suzuki, M. Tsutsui, D. Miura, S. Kurokawa, and A. Sakai, Jpn. J. Appl. Phys. (Part 1) **46**, 3694 (2007).
[4] T. Kizuka, Phys. Rev. B **77**, 155401 (2008).
[5] Y. Oshima, Y. Kurui, and K. Takayanagi, J. Phys. Soc. Jpn. **79**, 054702 (2010).
[6] E. Scheer *et al.*, Nature **394**, 154 (1998).
[7] Y. Kurui, Y. Oshima, M. Okamoto, and K. Takayanagi, Phys. Rev. B **79**, 165414 (2009).
[8] R. H. M. Smit, C. Untiedt, G. Rubio-Bollinger, R. C. Segers, and J. M. van Ruitenbeek, Phys. Rev. Lett. **91**, 076805 (2003).
[9] M. Dreher, F. Pauly, J. Heurich, J. C. Cuevas, E. Scheer, and P. Nielaba, Phys. Rev. B **72**, 75435 (2005).
[10] H. Ohnishi, Y. Kondo, and K. Takayanagi, Nature **395**, 780 (1998).
[11] F. Tavazza, L. E. Levine, and A. M. Chaka, J. Appl. Phys. **106**, 43522 (2009).
[12] N. Agraıt, A. L. Yeyati, and J. M. van Ruitenbeek, Phys. Rep. **377**, 81 (2003).
[13] N. Agraıt, G. Rubio, and S. Vieira, Phys. Rev. Lett. **74**, 3995 (1995).
[14] G. Rubio-Bollinger, P. Joyez, and N. Agraıt, Phys. Rev. Lett. **93**, 116803 (2004).
[15] A. Nitzan and M. A. Ratner, Science **300**, 1384 (2003).
[16] Z. Qian, R. Li, S. Hou, Z. Xue, and S. Sanvito, J. Chem. Phys. **127**, 194710 (2007).
[17] M. Brandbyge, J. L. Mozoz, P. Ordejon, J. Taylor, and K. Stokbro, Phys. Rev. B **65**, 165401 (2002).
[18] Y. Fujimoto and K. Hirose, Phys. Rev. B **67**, 195315 (2003).
[19] Y. J. Lee *et al.*, Phys. Rev. B **69**, 125409 (2004).
[20] M. Zhuang and M. Ernzerhof, J. Chem. Phys. **120**, 4921 (2004).
[21] A. Grigoriev *et al.*, Phys. Rev. Lett. **97**, 236807 (2006).
[22] L. Ke *et al.*, Nanotechnology **18**, 095709 (2007).
[23] S Barzilai, F. Tavazza, and L. E. Levine, Modelling Simul. Mater. Sci. Eng. **21**, 025004 (2013).
[24] F. Tavazza, L. E. Levine, and A. M. Chaka, Phys. Rev. B **81**, 235424 (2010).
[25] F. Tavazza, D. T. Smith, L. E. Levine, J. R. Pratt, and A. M. Chaka, Phys Rev. Lett. **107**, 126802 (2011).
[26] T. Shiota, A. I. Mares, A. M. C. Valkering, T. H. Oosterkamp, and J. M. van Ruitenbeek, Phys. Rev. B **77**, 125411 (2008).
[27] G. Robio-Bollinger, C. de las Heras, E. Bascones, N. Agrait, F. Guinea, and S. Vieira, Phys. Rev. B. **67**, 121407 (2003).
[28] D. Szczesniak and A. Khater, Eur. Phys. J. B **85**, 174 (2012)
[29] T. Kwapinski, J. Phys. Condens. Matter **22**, 295303 (2010).
[30] C. Bruot, J. Hihath, and N. Tao, Nature Nanotechnology **7**, 35 (2012).
[31] Commercial software is identified to specify procedures. Such identification does not imply recommendation by the National Institute of Standards and Technology.
[32] B. Delley, J. Chem. Phys. **92**, 508 (1990).
[33] B. Delley, J. Chem. Phys. **113**, 7756 (2000).
[34] S. Datta, *Electron Transport in Mesoscopic Systems* (Cambridge University Press, Cambridge, England, 1995).
[35] Atomistix ToolKit version 10.02, QuantumWise A/S.
[36] J. Taylor, H. Guo, and J. Wang, Phys. Rev. B **63**, 245407 (2001).
[37] J. P. Perdew, S. Burke, and M. Ernzerhof, Phys. Rev. Lett. **77**, 3865 (1996).
[38] B. Delley, Phys. Rev. B **66**, 155125 (2002).
[39] P. Pulay and G. Fogarasi, J. Chem. Phys. **96**, 2856 (1992).
[40] J. Baker, A. Kessi, and B. Delley, J. Chem. Phys. **105**, 192 (1996).
[41] H. J. Monkhorst and J. D. Pack, Phys. Rev. B **13**, 5188 (1976).
[42] J. P. Perdew and A. Zunger, Phys. Rev. B **23**, 5048 (1981).
[43] J. M. Soler, E. Artacho, J. D. Gale, A. Garc'ia, J. Junquera, P. Ordej'on, and D. S'anchez, J. Phys. Condens. Matter **14**, 2745 (2002).
[44] F. Tavazza, L. E. Levine, and A. M. Chaka, Modelling Simul. Mater. Sci. Eng. **19**, 074001 (2011).
[45] D. T. Smith, J. R. Pratt, F. Tavazza, L. E. Levine, and A. M. Chaka, J. Appl. Phys. **107**, 084307 (2010).
[46] D. T. Smith, J. R. Pratt, and L. P. Howard, Rev. Sci. Instrum. **80**, 035105 (2009).